Experiments on second- and third-harmonic generation from magnetic metamaterials

Matthias W. Klein and Martin Wegener

Institut für Angewandte Physik and DFG-Center for Functional Nanostructures (CFN), Universität Karlsruhe (TH), Wolfgang-Gaede-Straße 1, D-76131 Karlsruhe, Germany

Nils Feth and Stefan Linden

Institut für Nanotechnologie, Forschungszentrum Karlsruhe in der Helmholtz-Gemeinschaft, Postfach 3640, D-76021 Karlsruhe, Germany

Nils.Feth@physik.uni-karlsruhe.de

Abstract: Photonic metamaterials could provide optical nonlinearities far exceeding those of natural substances due to the combined action of (magnetic) resonances and local-field enhancements. Here, we present our experiments on second- and third-harmonic generation from magnetic metamaterials composed of nanoscale gold split-ring resonators and from control samples for excitation with 170-fs pulses centered at 1.5-μm wavelength. The strongest nonlinear signals are found for resonances with magnetic-dipole character.

OCIS codes: (160.4330) Nonlinear optical materials; (190.3970) Microparticle nonlinear optics; (260.5740) Resonance.

References and links

1. J. E. Sipe and R. W. Boyd, "Nonlinear susceptibility of composite optical materials in the Maxwell Garnett model," Phys. Rev. A **46**, 1614–1629 (1992).
2. G. L. Fischer, R. W. Boyd, R. J. Gehr, S. A. Jenekhe, J. A. Osaheni, J. E. Sipe, and L. A. Weller-Brophy, "Enhanced nonlinear optical response from composite materials," Phys. Rev. Lett. **74**, 1871–1874 (1995).
3. V. M. Shalaev, "Electromagnetic properties of small-particle composites," Phys. Rep. **272**, 61–137 (1996).
4. L. L. Beecroft and C. K. Ober, "Nanocomposite materials for optical applications," Chem. Mater. **9**, 1302–1317 (1997).
5. V. M. Shalaev and A. K. Sarychev, "Nonlinear optics of random metal-dielectric films," Phys. Rev. B **57**, 13265–13288 (1998).
6. J. B. Pendry, A. J. Holden, D. J. Robbins, and W. J. Stewart, "Magnetism from conductors and enhanced nonlinear phenomena," IEEE Trans. Microwave Theory Tech. **47**, 2075–2084 (1999).
7. J. B. Pendry, A. J. Holden, W. J. Stewart, and I. Youngs, "Extremely low frequency plasmons in metallic mesostructures," Phys. Rev. Lett. **76**, 4773–4776 (1996).
8. R. A. Shelby, D. R. Smith, and S. Schultz, "Experimental verification of a negative index of refraction," Science **292**, 77–79 (2001).
9. T. J. Yen, W. J. Padilla, N. Fang, D. C. Vier, D. R. Smith, J. B. Pendry, D. N. Basov, and X. Zhang, "Terahertz magnetic response from artificial materials," Science **303**, 1494–1496 (2004).
10. S. Linden, C. Enkrich, M. Wegener, J. Zhou, Th. Koschny, and C. M. Soukoulis "Magnetic response of metamaterials at 100 terahertz," Science **306**, 1351–1353 (2004).
11. S. Zhang, W. Fan, B. K. Minhas, A. Frauenglass, K. J. Malloy, and S. R. J. Brueck, "Midinfrared resonant magnetic nanostructures exhibiting a negative permeability," Phys. Rev. Lett. **94**, 037402 (2005).
12. C. Enkrich, M. Wegener, S. Linden, S. Burger, L. Zschiedrich, F. Schmidt, J. Zhou, Th. Koschny, and C. M. Soukoulis, "Magnetic metamaterials at telecommunication and visible frequencies," Phys. Rev. Lett. **95**, 203901 (2005).
13. G. Dolling, C. Enkrich, M. Wegener, J. Zhou, C. M. Soukoulis, and S. Linden, "Cut-wire pairs and plate pairs as magnetic atoms for optical metamaterials," Opt. Lett. **30**, 3198–3200 (2005).
14. N. Feth, C. Enkrich, M. Wegener, and S. Linden, "Large-area magnetic metamaterials via compact interference lithography," Opt. Express **15**, 501–507 (2007).
15. S. Zhang, W. Fan, N. C. Panoiu, K. J. Malloy, R. M. Osgood, and S. R. J. Brueck, "Experimental demonstration of near-infrared negative-index metamaterials," Phys. Rev. Lett. **95**, 137404 (2005).

#79550 - $15.00 USD Received 30 Jan 2007; revised 28 Mar 2007; accepted 4 Apr 2007; published 13 Apr 2007

16. V. M. Shalaev, W. Cai, U. K. Chettiar, H.-K. Yuan, A. K. Sarychev, V. P. Drachev, and A. V. Kildishev, "Negative index of refraction in optical metamaterials," Opt. Lett. **30**, 3356–3358 (2005).
17. G. Dolling, C. Enkrich, M. Wegener, C. M. Soukoulis, and S. Linden, "Simultaneous negative phase and group velocity of light in a metamaterial," Science **312**, 892–894 (2006).
18. G. Dolling, C. Enkrich, M. Wegener, C. M. Soukoulis, and S. Linden, "Low-loss negative-index metamaterial at telecommunication wavelengths," Opt. Lett. **31**, 1800–1802 (2006).
19. G. Dolling, M. Wegener, C. M. Soukoulis, and S. Linden, "Negative-index metamaterial at 780nm wavelength," Opt. Lett. **32**, 53–55 (2007).
20. V. M. Shalaev, "Optical negative-index metamaterials," Nat. Phot. **1**, 41–48 (2007).
21. C. M. Soukoulis, S. Linden, and M. Wegener, "Negative refraction at optical wavelengths," Science **315**, 47–49 (2007).
22. A. A. Zharov, I. V. Shadrivov, and Y. S. Kivshar, "Nonlinear properties of left-handed metamaterials," Phys. Rev. Lett. **91**, 037401 (2003).
23. S. O'Brien, D. McPeake, S. A. Ramakrishna, and J. B. Pendry, "Near-infrared photonic band gaps and nonlinear effects in negative magnetic metamaterials," Phys. Rev. B **69**, 241101 (2004).
24. A. K. Popov, V. V. Slabko, and V. M. Shalaev, "Second-harmonic generation in left-handed metamaterials," Las. Phys. Lett. **3**, 293–297 (2006).
25. A. K. Popov and V. M. Shalaev, "Negative-index metamaterials: second-harmonic generation, Manley-Rowe relations and parametric amplifications," Appl. Phys. B **84**, 131–137 (2006).
26. A. K. Popov and V. M. Shalaev, "Compensating losses in negative-index metamaterials by optical parametric amplification," Opt. Lett. **31**, 2169–2171 (2006).
27. M. V. Gorkunov, I. V. Shadrivov, and Y. S. Kivshar, "Enhanced parametric processes in binary metamaterials," Appl. Phys. Lett. **88**, 71912 (2006).
28. A. A. Zharov, N. A. Zharova, I. V. Shadrivov, and Y. S. Kivshar, "Subwavelength imaging with opaque nonlinear left-handed lenses," Appl. Phys. Lett. **87**, 091104 (2005).
29. R. S. Bennink, Y.-K. Yoon, and R. W. Boyd, "Accessing the optical nonlinearity of metals with metal-dielectric photonic bandgap structures," Opt. Lett. **24**, 1416–1418 (1999).
30. J. P. Huang, L. Dong, and K. W. Yu, "Giant enhancement of optical nonlinearity in multilayer metallic films," J. Appl. Phys. B **99**, 053503 (2006).
31. M. W. Klein, C. Enkrich, M. Wegener, and S. Linden, "Second-harmonic generation from magnetic metamaterials," Science **313**, 502–504 (2006).
32. R. W. Boyd, *Nonlinear Optics* (Academic, New York, 1992).
33. C. Rockstuhl, F. Lederer, C. Etrich, Th. Zentgraf, J. Kuhl, and H. Giessen, "On the reinterpretation of resonances in split-ring-resonators at normal incidence," Opt. Express **14**, 8827–8836 (2006).
34. G. Dolling, M. Wegener, and S. Linden, "Realization of a three-functional-layer negative-index photonic metamaterial," Opt. Lett. **32**, in press (2007).

1. Introduction

It is one of the dreams of scientists working in the field of nonlinear optics to custom-design nonlinear-optical materials with nonlinear coefficients largely outperforming those of natural crystals, thereby further enlarging the applications of nonlinear optics [1–6]. In *linear optics*, the ability of tailoring material properties to such unprecedented degree is presently becoming reality with the introduction of metamaterials [6–8]. Photonic metamaterials are man-made materials composed of nanostructured subwavelength metallic building blocks ("photonic atoms") that are densely packed into an effective optical material. Ideally, the metamaterial "lattice constant" is much smaller than the wavelength of light. Along these lines, magnetism at optical frequencies [9–14] and a negative index of refraction at optical frequencies [15–18] and the red end of the visible [19] have become possible experimentally. References [20,21] are recent reviews. Regarding *nonlinear optics* with metamaterials, several theoretical papers have highlighted new options regarding optical bistability [22,23], second-harmonic generation [24,25], parametric nonlinear processes [26,27], and nonlinear subwavelength imaging [28]. Most of these theoretical papers start from effective nonlinear coefficients. However, a consistent microscopic theory allowing to compute these nonlinear coefficients of photonic metamaterials has not been published so far. Obviously, such theory with predictive power would be extremely helpful if not crucial to actually custom-design nonlinear-optical materials in experiments. Conversely, to test such theory, experimental data are essential. Currently, the subfield of nonlinear optics of photonic metamaterials is just at its beginning,

#79550 - $15.00 USD Received 30 Jan 2007; revised 28 Mar 2007; accepted 4 Apr 2007; published 13 Apr 2007

being short of both, experiment and microscopic theory. (One-dimensional metal/dielectric stacks are an exception, for example see references [29,30].) It is the aim of this article to contribute to the experimental part.

Much of the emerging field of photonic metamaterials has been stimulated by the 1999 work of John Pendry et al. [6] that addressed magnetic split-ring resonators (SRRs), providing artificial magnetism up to optical frequencies. In essence, a SRR is just a subwavelength metallic ring with a slit. The light field can induce a circulating current in the ring that leads to a large magnetic-dipole moment close to the magnetic-resonance frequency. In addition, the same article also suggested the possibility of enhanced nonlinear-optical effects from metamaterials composed of SRRs due to the combined presence of resonances and local-field enhancements. Corresponding experiments on second-harmonic generation (SHG) under normal incidence on gold SRRs have recently been presented by us [31]. Here, we provide additional experimental data which might eventually help elucidating the underlying not-well-understood microscopic mechanism by quantitative comparison with microscopic theories which are presently not available.

2. Metamaterial fabrication

All metamaterial samples discussed in this article have been fabricated by standard electron-beam lithography, high-vacuum electron-beam evaporation of the gold the SRRs are composed of, and a lift-off procedure. Details on the fabrication can be found in our references [12,13]. The magnetic metamaterials exhibit different resonances with magnetic- and/or electric-dipole character. Obviously, it is interesting to compare the nonlinearities of these different resonances. At first sight, tuning of the incident laser seems to be a good choice. However, the different resonances are separated by as much as a factor of two in wavelength. Thus, the gold optical nonlinearities would likely change considerably, even interband transitions in the gold will come into play at short wavelengths. Thus, we rather keep the excitation wavelength fixed and lithographically tune the metamaterial resonances by adjusting the SRR size. It is well known that for frequencies far below the metal plasma frequency, the SRR resonance wavelengths are simply proportional to the SRR size. Importantly, we fabricate sets of different samples (each 100μm×100μm footprint) in one fabrication run on the same glass substrate. This step ensures that it is really meaningful to compare the nonlinear-optical signal strengths of different samples.

3. Second- and third-harmonic generation from SRRs under normal incidence

In our nonlinear-optical experiments under ambient conditions, we excite the metamaterial samples under normal incidence with 170fs Gaussian pulses derived from an optical parametric oscillator (Spectra Physics OPAL, 81MHz repetition frequency) tuned to 1.5μm center wavelength. The linear polarization of the incident light can be adjusted by a polarizer and a half-wave plate. Typically, 50mW of average power are focused to a Gaussian spot on the sample with 60μm in diameter (as measured by a knife-edge technique). From these numbers, we estimate an incident peak electric-field of 2×10^7V/m. The transmitted light is collimated with a lens, spectrally filtered (either for the second harmonic or the third harmonic, respectively), is sent through a second polarizer for analysis, and is finally detected by a photomultiplier tube. We have checked that the nonlinear signal actually scales with the incident intensity to the power of two (three) for the second (third) harmonic (not shown).

Figure 1 summarizes results on second-harmonic generation (SHG) and third-harmonic generation (THG). Electron micrographs of the samples are shown in the left-hand side column, the gold thickness is 25nm. In (a) and for horizontal incident polarization, the fundamental magnetic-dipole resonance of the SRRs is resonantly excited [12] and the strongest SHG and THG signals are found. We normalize these two signals to 100% and relate all other signals to these cases (the noise level corresponds to about 0.3% and 0.4% for SHG and THG, respectively). This normalization must not be confused with the absolute conversion efficiencies.

#79550 - $15.00 USD Received 30 Jan 2007; revised 28 Mar 2007; accepted 4 Apr 2007; published 13 Apr 2007

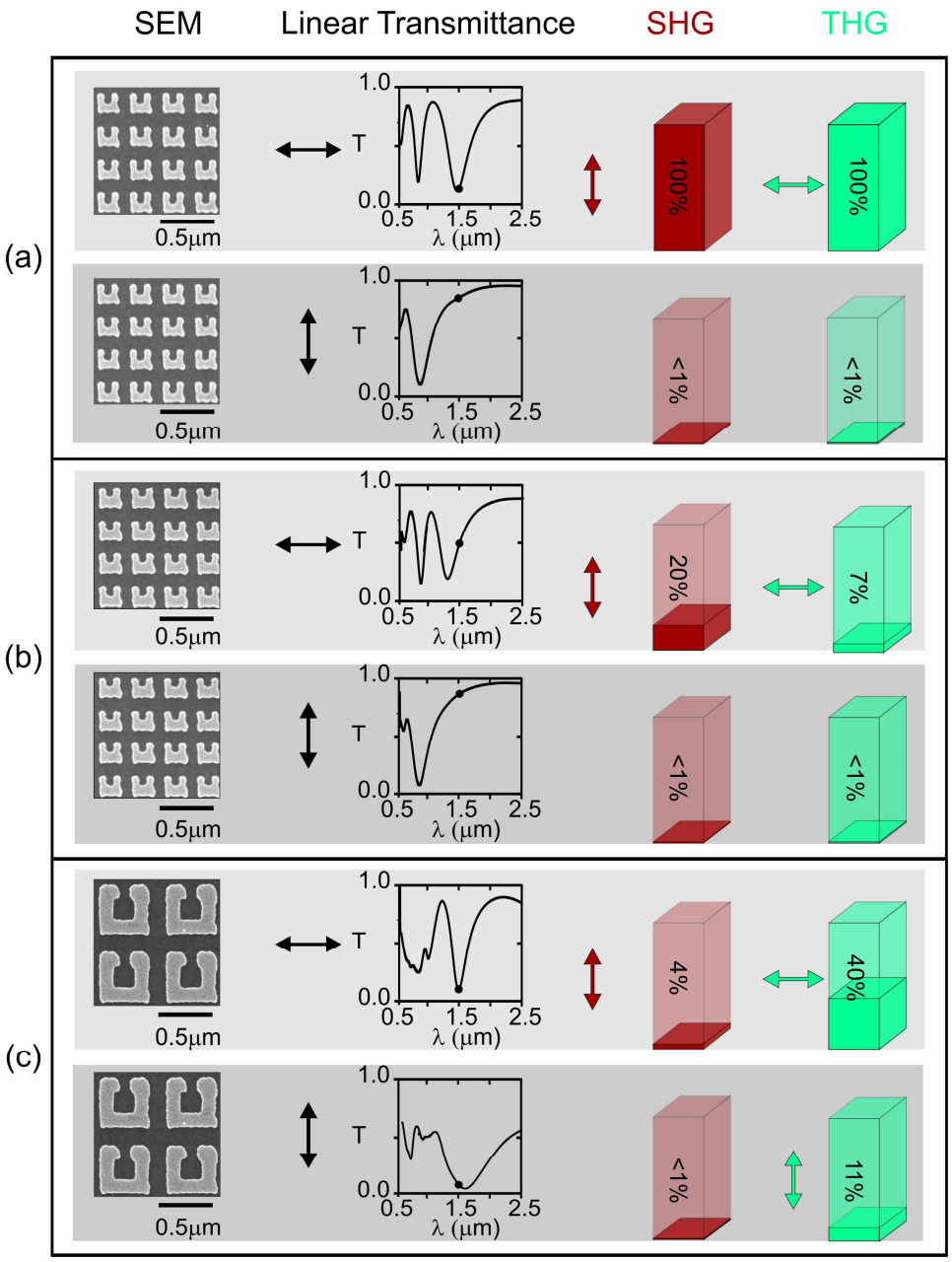

Fig. 1. Experiments on three different samples: (a) small SRRs with a fundamental magnetic resonance centered at 1.5µm wavelength, (b) a slightly detuned structure, and (c) large SRRs with a higher-order resonance around 1.5µm. For each case, the two linear polarizations are shown (horizontal on top, vertical at bottom). The different columns (from left to right) show electron micrographs, measured linear transmittance spectra, measured SHG signal strength for excitation centered at 1.5µm wavelength, and corresponding THG signal strength. The arrows indicate the incident linear polarization (black), the measured linear polarization of the SHG (red), and that of the THG (green) – if sufficiently large. For clarity, the nonlinear signals are normalized to (a), horizontal incident polarization.

#79550 - $15.00 USD Received 30 Jan 2007; revised 28 Mar 2007; accepted 4 Apr 2007; published 13 Apr 2007

From the measured signal, the specified photomultiplier quantum efficiency, and from a correction for all optical components in the optical pathway we roughly estimate an absolute conversion efficiency of 2×10^{-6} for the SHG and 3×10^{-7} for the THG under these conditions. A corresponding 25-nm-thin film of a standard nonlinear-optical material would deliver yet much smaller SHG signals. For example, for potassium dideuterium phosphate (KDP) with $\chi^{(2)}= 1.0\times10^{-12}$m/V [32], we estimate a SHG conversion efficiency on the order of 10^{-11} under these conditions. From a closed gold film of the same thickness on the identical glass substrate we find no SHG (as expected from symmetry) and no THG signal for normal incidence. Also, no measurable SHG signal is found for oblique incidence in p-polarization for angles up to 60 degrees with respect to the surface normal. For the latter case, symmetry would allow for SHG. Exciting the same SRRs with vertical linear incident polarization [bottom row of Fig. 1(a)] leads to no significant SHG and THG signals.

The structures in Fig. 1(b) are effectively detuned with respect to those in (a) by 0.25μm in wavelength. Clearly, the SHG signal decreases from 100% to 20% for excitation in the long-wavelength wing of the resonance and horizontal incident polarization. Correspondingly, the THG decreases from 100% to 7%. This comparison shows that the nonlinear signals are resonantly enhanced – as expected. Again, no significant SHG and THG signals are found for vertical incident polarization.

In Fig. 1(c), we excite a higher-order resonance of much larger SRRs, again with horizontal incident polarization. This configuration leads to a signal strength for SHG (THG) of 4% (40%). Interestingly, this resonance also reveals a magnetic-dipole moment originating from a higher-order magnetic resonance that has been discussed in references [12,33]. In essence, the electric current mode of this resonance can be interpreted as a standing current wave on the ring with two nodes and three antinodes. Finally, we again find lower signals for vertical incident polarization.

4. Second- and third-harmonic generation from control samples under normal incidence

Is the observed enhancement of SHG and THG just a combination of resonant effects and appropriate symmetry or is there something special about the magnetic-dipole character of particular resonances? To address this question, we have fabricated an additional set of samples (again, all fabricated in one run on one substrate), the results of which are summarized in Fig. 2. Here, we compare excitation of the fundamental magnetic resonance of the SRRs [as in Fig. 1(a)] with two other structures. One control structure [Fig. 2(b)] is an array of straight cut wires, which can be viewed as stretched-out versions of the SRRs. From centro-symmetry, no SHG is expected and, indeed, no significant SHG is found. This observation indicates that the measured nonlinear signals are not dominated by extrinsic effects, like "hot spots." The second control sample [Fig. 2(c)] consists of "T"-shaped structures without centro-symmetry, allowing for SHG. Nevertheless, the SHG signal is within the noise – even though a resonance is excited. Clearly, both the cut wires and the "T"-structures exhibit zero magnetic-dipole moment. The combination of these observations suggests that the measured large SHG signals from the magnetic resonances of the SRRs are connected to the magnetic-dipole character of these resonances. The THG signals from these control samples are also shown in Fig. 2 for completeness.

5. Second-harmonic generation from SRRs under oblique incidence

Next, we present experimental data on SHG from SRRs excited under oblique incidence. Clearly, the spot size on the sample increases with increasing angle α with respect to the surface normal. Due to the finite sample size (100μm×100μm), this effect limits the experimentally accessible angles to a maximum of about α = 60 degrees. At 60 degrees, the Gaussian spot diameter ($1/e^2$ diameter of the intensity profile) increases from 60μm to 120μm, but the squared Gaussian profile ($120\mu m/\sqrt{2}\approx85\mu m$) relevant for the SHG is still smaller than the sample size. Hence, we do not expect major distortions. Also, it should be clear that

#79550 - $15.00 USD Received 30 Jan 2007; revised 28 Mar 2007; accepted 4 Apr 2007; published 13 Apr 2007

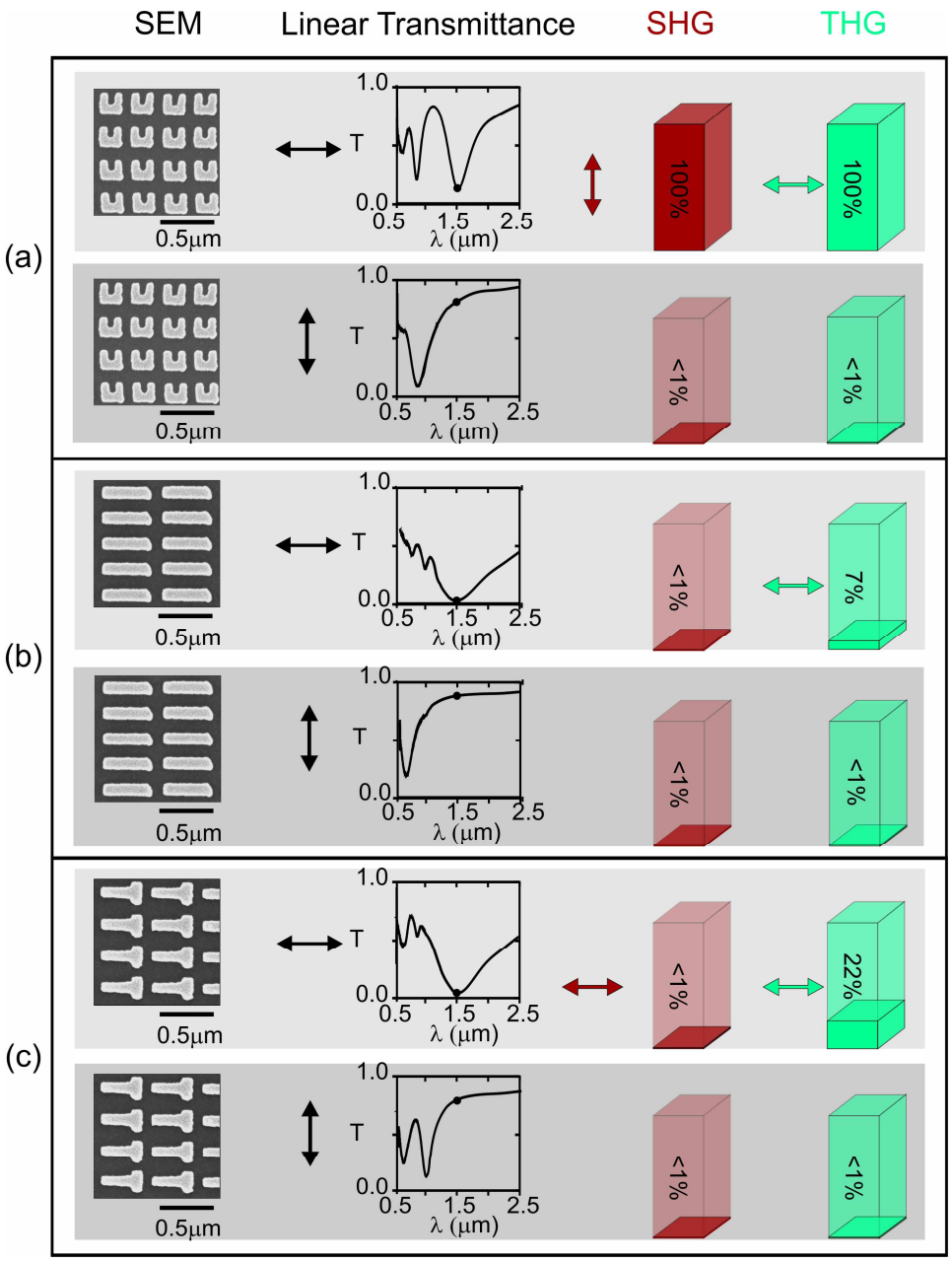

Fig. 2. Experiments on control samples: (a) similar (but not identical) to Fig. 1(a), (b) metamaterial composed of single cut wires, and (c) metamaterial composed of "T"-structures. The representation is as in Fig. 1.

#79550 - $15.00 USD Received 30 Jan 2007; revised 28 Mar 2007; accepted 4 Apr 2007; published 13 Apr 2007

positive and negative angles α are not always necessarily equivalent because of the low symmetry of the SRRs (see below). Thus, we measure SHG for both positive and negative angles.

We restrict ourselves to two different SRR sizes for which either the fundamental magnetic resonance [see Fig. 1(a)] or a higher-order resonance wavelength [see Fig. 1(c)], respectively, coincides with the incident laser wavelength. For each of these two samples, we have two orthogonal incident linear polarizations and two orthogonal axes of sample rotation, hence eight different geometries, six of which are resonant and depicted in Figs. 3 and 4. For reference, corresponding linear-optical transmittance spectra are shown in Fig. 3. The geometries are illustrated by the nearby schemes. These spectra are taken with a dedicated home-built setup [12] allowing for oblique-incidence spectroscopy on small-area samples at an opening angle of the incident light of about five degrees (whereas the transmittance spectra in Figs. 1 and 2 are recorded with a commercial Fourier-transform microscope-spectrometer, Bruker Equinox 55 and Bruker Hyperion 2000, numerical aperture NA=0.5). The spectra are normalized with respect to the bare substrate for the same angle of incidence. The underlying physics has been discussed in reference [12].

Results regarding SHG are summarized in Fig. 4. Obviously, the data are quite complex and we are presently unable to explain them in detail. However, a few aspects are clear. (i) The SHG signals for all geometries and angles α are smaller than for normal-incidence excitation of the fundamental magnetic resonance with horizontal incident polarization [see Fig. 1(a)] – the 100% signal. (ii) The SHG signal from this resonance decreases with increasing angle $|\alpha|$, while the fundamental magnetic resonance can still be excited, as apparent from the linear transmittance spectra (see Fig. 3). In contrast, the SHG signal for the other sample composed of large SRRs initially increases with increasing angle $|\alpha|$ before it reaches a maximum. (iii) We do observe significant differences of the SHG signals between positive and negative angles for some geometries (see Fig. 4), while the linear-optical transmittance spectra (see Fig. 3) show no significant differences between positive and negative angles, respectively. For s-polarization, the differences in Fig. 4(b) and (c) are consistent with the assumption that the magnetic-field component of the incident light field plays a role. Its component normal to the SRR plane changes sign when going from positive to negative angles α. The corresponding differences in the SHG signals for p-polarization in Fig. 4(b) are likely due to the fact that the SRRs deviate from perfect vertical mirror symmetry. (iv) Beyond these points (i)-(iii), a detailed interpretation of the SHG signals from the large SRRs is complicated by the fact that the resonance positions shift and split with increasing angle $|\alpha|$ with respect to the fixed excitation wavelength (see Fig. 3).

6. Discussion and conclusions

We have presented an experimental study of SHG and THG from metamaterials composed of split-ring resonators as well as from other photonic metamaterials serving as control samples. We find a positive correlation of nonlinear signal strength and magnetic-dipole character of resonances. Unfortunately, we are presently not in the position to compare these experimental results to a complete microscopic theory of the optical nonlinearities from photonic metamaterials. It is well known that the optical nonlinearities of metals are orders of magnitude larger than those of typical dielectrics. Under our conditions, quantum effects of metal electrons are not expected to be relevant. Thus, we assume that a classical description of plasma nonlinearities is an adequate starting point: One has to solve self-consistently Newton's law for metal electrons with an electric and a magnetic component of the Lorentz force and the Maxwell equations for the metallic nanostructure. The charge density at the fundamental frequency does not change in the volume of the metal. Thus, the current density at the second-harmonic frequency associated with the electric component of light is only nonzero on the metal surface. In contrast, the second-harmonic current density due to the magnetic component of the Lorentz force is a volume term. In our recent work [31], we have

#79550 - $15.00 USD Received 30 Jan 2007; revised 28 Mar 2007; accepted 4 Apr 2007; published 13 Apr 2007

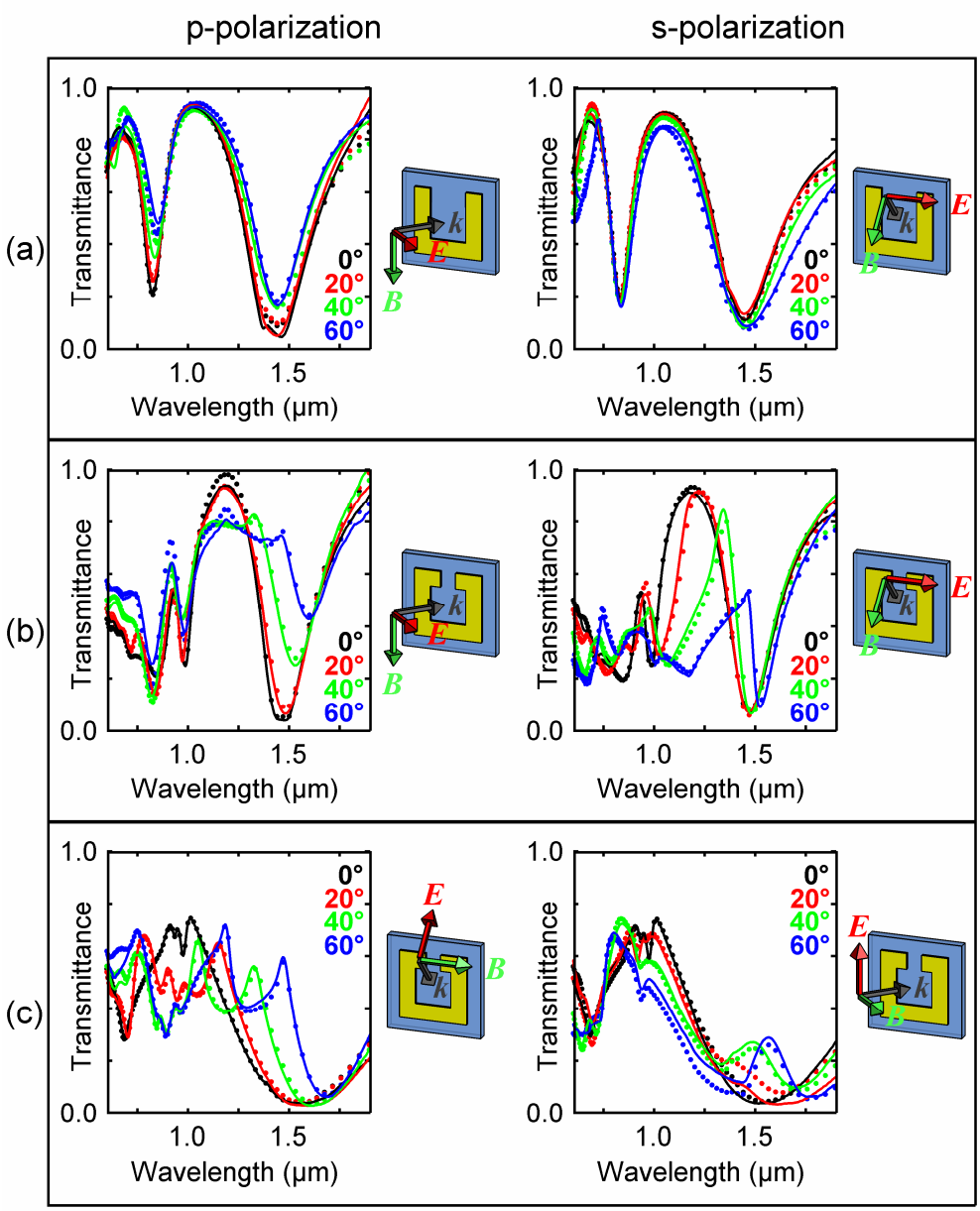

Fig. 3. Oblique-incidence transmittance spectra of two samples. Row (a) corresponds to the sample in Fig. 1(a), rows (b) and (c) to that in Fig. 1(c). The angle of incidence with respect to the surface normal is indicated by the color, positive angles (solid curves) and negative angles (dots) are depicted. The left column corresponds to p-polarization, the right column to s-polarization. The polarization geometries (for positive angles) are also illustrated by the insets.

#79550 - $15.00 USD Received 30 Jan 2007; revised 28 Mar 2007; accepted 4 Apr 2007; published 13 Apr 2007

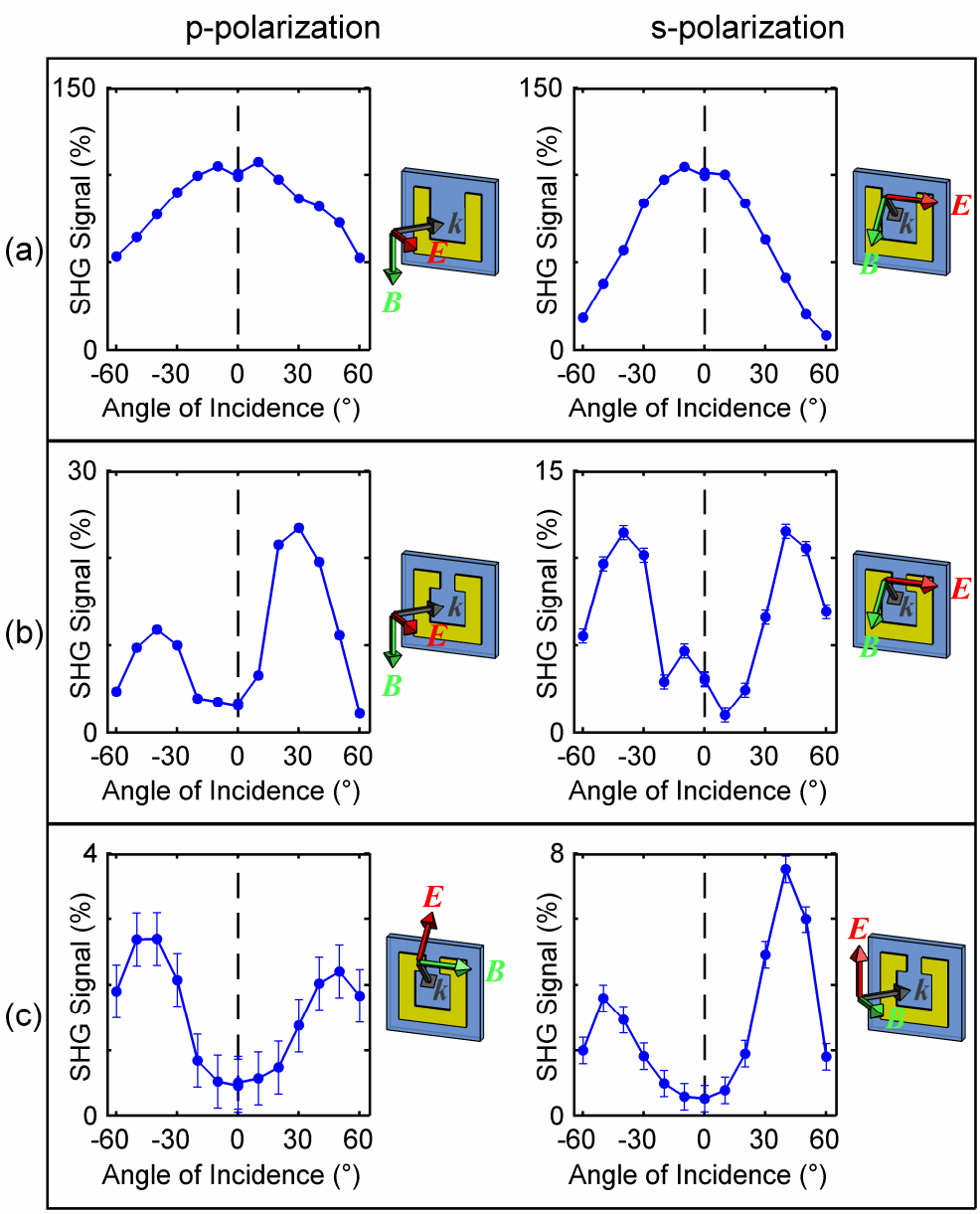

Fig. 4. SHG signal strength obtained from SRRs excited under oblique incidence as a function of the angle of incidence α with respect to the surface normal. The samples and geometries directly correspond to those shown in Fig. 3. For convenience, the excitation geometries are again illustrated here. All SHG signal strengths are normalized to that for normal incidence in Fig. 1(a), horizontal incident linear polarization. Note the different SHG signal scales.

#79550 - $15.00 USD Received 30 Jan 2007; revised 28 Mar 2007; accepted 4 Apr 2007; published 13 Apr 2007

shown that the latter mechanism is consistent with the SHG data. This finding, however, is by no means a proof that this contribution dominates. Thus, especially more theoretical work in this direction is necessary. The experimental data presented here can provide a sensitive test ground for such theories.

Broadly speaking, the spirit of the emerging field of photonic metamaterials is to design and fabricate artificial tailored optical materials exhibiting linear- and/or nonlinear-optical properties that simply do not occur in natural substances. Regarding nonlinear optics, one obvious concrete goal is to increase effective nonlinear-optical coefficients by orders of magnitude. For very thin films, the magnetic metamaterials presented in this article already outperform standard SHG materials by orders of magnitude with respect to conversion efficiency. Clearly, the future challenge is to extend this success to larger and especially to thicker metamaterial structures in order to become meaningful for applications. Such three-dimensional (rather than planar) photonic metamaterials are elusive to date, while first steps in this direction have been taken [34]. In that context, the problems of absorption and phase-matching would have to be solved.

Acknowledgments

We thank the groups of Costas M. Soukoulis, Stephan W. Koch, and Jerome V. Moloney for discussions. Harald Giessen and Teruya Ishihara suggested the experiments on control samples. We acknowledge support by the Deutsche Forschungsgemeinschaft (DFG) and the State of Baden-Württemberg through the DFG-Center for Functional Nanostructures (CFN) within subproject A1.5. This work is embedded in the Karlsruhe School of Optics & Photonics (KSOP). The research of S. L. is further supported through a “Helmholtz-Hochschul-Nachwuchsgruppe” (VH-NG-232).

#79550 - $15.00 USD Received 30 Jan 2007; revised 28 Mar 2007; accepted 4 Apr 2007; published 13 Apr 2007